

Evaluation of nonlinear numerical model performance on the wave propagation over a bar-trough profile beach

T. Okamoto[†], C.J. Fortes[†] and M.G. Neves[†]

[†]Harbors and Maritime structures Division, Department of Hydraulics and Environmental, Lisbon, 1700-066, Portugal, [tokamoto, jfortes, gneves]@lnec.pt



ABSTRACT

OKAMOTO, T., Fortes, C.J. and Neves, M.G. 2009. Evaluation of nonlinear numerical model performance on the wave propagation over a bar trough profile beach. Journal of Coastal Research, SI 56 (Proceedings of the 10th International Coastal Symposium), pg – pg. Lisbon, Portugal, ISBN

Knowing the vertical structure of particle velocity is very important for the sediment transportation study. Recent development of computer resources and high performance computing enable us to use numerical models with more information in the vertical direction. In this paper, the performance of multi-layered Boussinesq model (COULWAVE) and RANS model (COBRAS-UC) on a bar-trough profile beach is examined. Results, in terms of wave heights computed by both models and the time series of the horizontal velocity (computed with COBRAS-UC model) are compared with the experimental data collected by Okamoto *et al.* (2008) for the test case with an incident wave of period $T=1.5$ sec and height of $H=8$ cm, in which the detailed vertical structure of particle velocity was measured. Both models can predict the wave height change very well until the wave breaking initiates and specially COBRAS-UC model. However, it does not agree to the experimental data after the wave breaking initiation. The COBRAS-UC model calculates the horizontal velocity near the free surface very well, but it does not agree to the experimental data in the lower section of the water column.

ADDITIONAL INDEX WORDS: *Wave breaking, Boussinesq type models, RANS model, Experimental work*

INTRODUCTION

Wave breaking is an important phenomenon in the nearshore region because the energy exerted from the breaking wave drives various nearshore phenomena, such as set-up/down, longshore current, nearshore circulation and so on. Therefore, accurate prediction of wave breaking area is the key in the coastal engineering project.

The Boussinesq-equation-based numerical has become a common analysis tool for the nearshore hydrodynamics in the last decade due to the development of computer power and the extension of the applicable limit. The wave breaking in this kind of models is reproduced by adding extra momentum terms to the momentum equation as a sink term to realize the energy dissipation due to the wave breaking. These extra momentum terms are only active during the wave breaking event and the decision for which wave is in the state of wave breaking is made by the external wave breaking index. The breaking model is controlled by empirical parameters that define the initiation, duration and termination of the wave breaking. The multi-layered Boussinesq equation model (LYNETT and LIU, 2004) is an example of this type of models. It uses for the vertical distribution of the flow field, quadratic polynomials, matched at the interface that divides the water column into layers. This approach leads to a set of model equations without the high-order spatial derivatives associated with high-order polynomial approximations usually employed in the common Boussinesq models. In this way, the model exhibits accurate linear characteristics up to a $kh \sim 8$ and nonlinear accuracy to $kh \sim 6$. Anyway, at each layer the vertical

flow field is approximated by a quadratic polynomial, so, it does not simulate correctly the vertical velocity profile.

This aspect is more important when the dealing with sediment transportation is considered, because simulating the vertical structure of particle velocity correctly is an important factor.

The Reynolds Averaged Navier-Stokes equation (RANS) models are often used in the CFD and show very good agreements with the experimental data. But it requires strong computational power as a practical tool.

In this paper, the performance of a multi-layered Boussinesq model (COULWAVE, LYNETT and LIU, 2004) and a RANS model (COBRAS-UC, LARA *et al.*, 2006) on a bar-trough profile beach. Wave heights and time series of the horizontal velocity are compared with experimental data from OKAMOTO *et al.* (2008), especially for the test case with an incident wave of period $T=1.5$ sec and height of $H=8$ cm, in which the detailed vertical structure of particle velocity was measured. The water depth at the top of the bar is 10 cm. The comparison contributes to a better understanding about the behavior of each numerical model on the inversed slope section.

Since COULWAVE is dependent on several parameters related to the wave breaking, a previously sensitivity analysis on the variation of the initiation parameter at COULWAVE model is also performed. This permit to find the parameter that best fit the experimental data. In the case of COBRAS-UC model, the turbulent model is based on the $k-\epsilon$ model and there is no parameter adjustment by user.

WAVE TANK EXPERIMENTS

Test conditions

Wave tank experiments were conducted at the National Laboratory of Civil Engineering (LNEC) in Lisbon, Portugal. Simplified bar-trough shaped beaches were installed as shown in Figure 1. Since the original bottom configuration of the tank is not a flat bottom, a wave gauge was installed at the toe of the front face of bar for checking the input wave condition. The wave tank does not have uniform width. The width of the tank varies from 0.95m at the toe of the slope to 0.60m at 2m before the bar crest. The width of the tank is uniform with 0.60m in the rest of area.

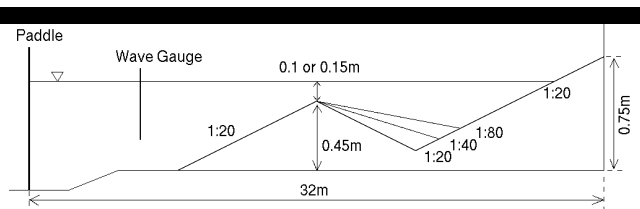


Figure 1. Bottom configuration of the wave tank.

Seven wave gauges were installed for the calculation of wave celerity and wave height in the area of measurement, which is from 200cm before the bar crest to the bottom of the trough. Wave gauges were separated with 20cm distance due to the instrumental restriction. Two series of measurements, such as $x=0, 20, 40, \dots$, cm and $x=10, 30, 50, \dots$, cm were conducted so that the resolution of data is 10cm (Figure 2 (a)). The natural oscillation of the wave tank was measured by taking the mean water level change. It was found that it takes, at least, about four minutes for the oscillation to become small enough. Therefore, the data collection was started to record after five minutes from the changing of input wave conditions. The duration of the record was two minutes and the sampling rate was 100Hz.



(a) Wave gauges

(b) ADV

Figure 2. Measurement equipments

For particle velocity measurements it was used an ADV mounted on an iron bar and placed at the location of interest as shown in Figure 2 (b). The particle velocity is not uniform over the water depth due to several reasons such as wave type (deep and intermediate water waves), undertow, bottom friction, and so on. Data obtained on a horizontal bottom (OKAMOTO and BASCO, 2006) suggested that the particle velocity at the middle of the water column shows close value against the average over the water depth, so that the probe of the ADV was positioned at around the middle of water column as a general rule. For some locations the velocity was measured at several water depths to check the velocity profile over the wave column. The sampling rate of the ADV was 25Hz, which is the maximum resolution the device can make.

Water depth was measured at the crest of the bar, $d=10$ and 15 cm. The four wave periods were tested in each water depth

condition. Four input wave heights (8, 10, 15, 20cm) for $d=10$ cm and two input wave heights (10 and 15cm) for $d=15$ cm were tested. Wave was broken at the paddle in one case due to the steepness condition, so total 69 cases were tested.

Wave heights

The wave heights were calculated from the wave gauge data by the down-crossing method. Set-up was not considered here so that the water depth is the still water depth.

Figure 3 displays the evolution of the relative wave height for all tested cases on 1/20 back slope. Up to certain point (around 0.8 on the relative distance scale), the relative wave height decreases asymptotically towards about 0.4. This is very similar to the decay equation for horizontal bottom given by DALLY *et al.* (1985). Then, the relative wave height once nearly stabilized starts to decrease again. The relative wave height at the termination location is 0.3 in average. The theory given by DALLY *et al.* (1985) cannot explain this second change near the termination.

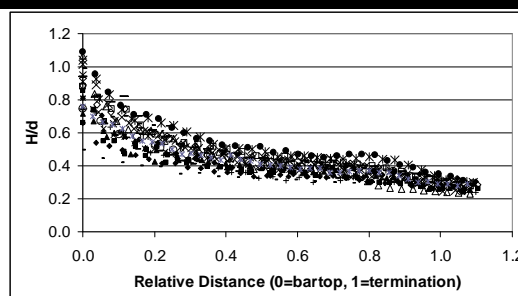


Figure 3. Relative wave height from the bar-top to the termination of wave breaking (1/20 back slope).

Figure 4 displays an example of the comparison of the wave height change with $d=10$ cm, $T=1.5$ sec, and $H=8$ cm for three different slopes at the lee side of the bar. The wave height changes in the front face of the bar (negative values in x-axis in Figure 4 are almost identical, which means the bathymetry change in the lee side of the bar does not affect to the wave before entering the trough region. This may sound obvious but it was necessary to be confirmed because of the nonlinear effects of the wave. Wave height in the trough region becomes bigger on steeper slope than on milder slope as shown in Figure 4.

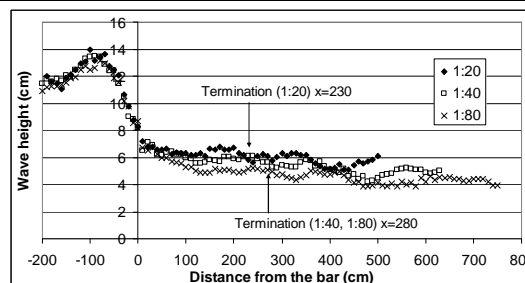


Figure 4. Comparison of the wave height change among different back slope settings ($d=10$ cm, $T=1.5$ sec, $H=8$ cm).

Particle velocity

Three representative values were calculated from the record. The maximum and minimum values were extracted for each one

wave period and made them averaged. The time average of whole record was considered the mean velocity. Figure 5 displays the mean, the minimum and the maximum velocity for $d=10\text{cm}$, $T=1.5\text{sec}$ and $H=8\text{cm}$ on $1/20$ back slope. The mean water flow is almost negligible before and after the wave breaking. But the mean water flow gives large influence on the particle velocity during the wave breaking. It becomes about the half of the contribution due to the wave motion in maximum. It is so strong that there is almost no flow in the on-shore direction at the area soon after the bar crest.

The mean water flow is mainly driven by the mean water level difference, such as set-up/down. But the minimum intensity of the crest velocity always appears soon after the crest of the bar, regardless of the initiation location of the wave breaking.

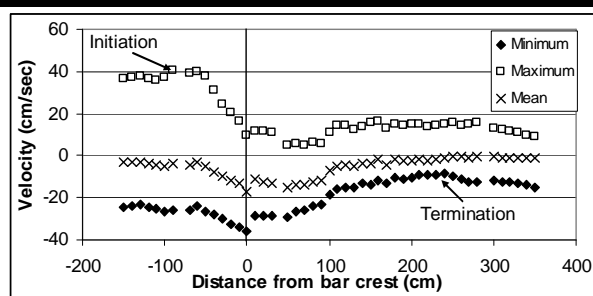


Figure 5. Mean water flow and the envelope of the particle velocity ($d=10\text{cm}$, $T=1.5\text{sec}$, $H=8\text{cm}$ on $1/20$ back slope)

The particle velocity was measured at every 1cm in depth at six locations for $d=10\text{cm}$, $T=1.5\text{sec}$, $H=8\text{cm}$ on $1/20$ back slope. Figure 6 displays the vertical structure of particle velocity at $x=-150\text{cm}$, where the wave breaking has not been initiated. This figure displays that there is a slight tendency of the mean water flow in the offshore direction throughout the water column, but the variation in the depth is very small. At $x=50\text{cm}$ where the strong mean flow is observed (See Figure 5), the mean particle velocity near the bottom is faster than the upper part of the water column. This suggests the existence of undertow but the variation in the vertical direction is relatively small comparing to the magnitude of mean flow.

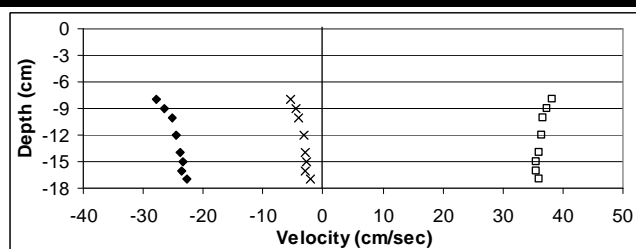


Figure 6. Vertical structure of particle velocity of $d=10\text{cm}$, $T=1.5\text{sec}$, $H=8\text{cm}$, $x=-150\text{cm}$.

NUMERICAL APPLICATIONS

The numerical wave calculations were performed with COULWAVE and COBRAS-UC models, for the test case of $d=10\text{cm}$, $T=1.5\text{sec}$, $H=8\text{cm}$ on a $1/20$ slope.

This particular case was chosen since a detailed vertical structure of particle velocity was measured in the physical tests.

The particle velocity was measured at 1cm each in depth, as much as the probe of ADV was completely submerged, at six locations from before the wave breaking to after the wave breaking.

For those conditions, wave heights with both models and velocities with COBRAS-UC model along the flume were calculated. Those values were compared with experimental ones. Previously, a sensitivity analysis was made for the establishment of the initiation breaking parameter at the COULWAVE model.

Numerical models description

COULWAVE (LYNETT and LIU, 2004) is a nonlinear wave propagation model based upon a multi layer approach for the integration of the primitive equations of motion (continuity and momentum equations). This approach leads to a set of model equations without the high-order spatial derivatives associated with high-order polynomial approximations.

The optimized model equations show good linear wave characteristics up to a kh of 8, while the second-order nonlinear behavior is well-captured to $kh \sim 6$. This is a greater than two-fold extension to higher kh over existing $O(1)$ Boussinesq-type. To enable the Boussinesq model to simulate surf zone hydrodynamics, energy dissipation due to wave breaking is treated by introducing an eddy viscosity term into the momentum equations, with the viscosity strongly localized on the front face of the breaking waves. Wave run-up on the beach is simulated using a permeable seabed technique. Both wave breaking and run-up schemes follow the work of KENNEDY *et al.* (2000).

By taking the volume-average of RANS equations, LIU *et al.* (1999) presented a two-dimensional numerical model, nicknamed COBRAS, to describe the flow inside and outside coastal structures including permeable layers. HSU *et al.* (2002) extended the preliminary model by including a set of volume-averaged $k-\epsilon$ turbulence balance equations. The movement of free surface is tracked by the Volume of Fluid (VOF) method. In the VARANS equations, the interfacial forces between the fluids and solids have been modeled by the extended Forchheimer relationship, in which both linear and nonlinear drag forces are included.

COBRAS-UC is a new version of the model developed at the University of Cantabria in order to overcome some of the initial limitations and especially to convert it into a tool for practical application. Most of these modifications in the new version COBRAS-UC have been founded on the extensive validation work carried out for low-crested structures (GARCIA *et al.* 2004, LOSADA *et al.* 2005 and LARA *et al.* 2006a) and wave breaking on permeable slopes (LARA *et al.* 2006b) carried out with the model. The improvements cover the wave generation process; code updating and re-factoring; optimization and improvement of the main subroutines; improvement of input and output data definition and the development of a graphical user interface and output data processing programs, LOSADA *et al.* (2007).

Numerical conditions and computational domain

In this study, COULWAVE model was used to calculate the free surface elevation and the wave heights for the case study, for the incident wave of $T=1.5\text{sec}$ and $H=0.08\text{m}$.

A section of the computational domain of COULWAVE model (in the x -direction is the same as the COBRAS-UC model) is presented in Figure 7. It is 32m long and 1m width. The bathymetry, reproduced as it happens in the physical model, was discretized with a spacing of $dx=0.05\text{m}$. The decrease on the width of the physical model was not simulated, due to the limitations of COULWAVE model. The COULWAVE model generates a finite difference grid based upon the minimum number of points per wavelength given by the user, which in this case

were 40. Two layers were considered on these calculations. The Courant number was equal to 0.1. Two absorbing boundaries were considered at the beginning and at the end of the domain with a length of one wave length. It was considered a friction coefficient equal to 1.0×10^{-2} .

The source function for the wave generation is located $x = 0.0\text{m}$.

The total simulation time was 300 s. For the remaining model parameters it was assumed, as a first approach, the values suggested in the COULWAVE model user's manual (LYNETT and LIU, 2002).

30 wave gauges were installed along the channel, being 8 of them at the same position of the physical model experiments (Figure 8).

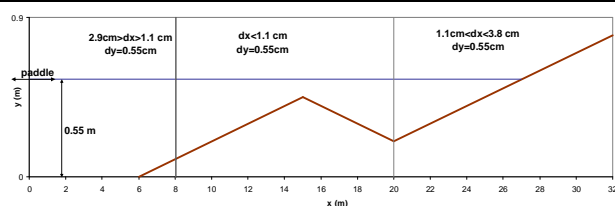


Figure 7. Computational domain of COULWAVE and COBRAS-UC models. Computational grid in the y-direction used in COBRAS-UC.

The model COBRAS-UC was used to calculate the surface elevation and the vertical profile of the horizontal velocity for the case study. The location, dimensions and characteristics of the experimental geometry were reproduced in the numerical model, shown as Figure 7. However, the position of the wave maker was not the same: the experimental flume is larger than the numerical one. Moreover, the reducing of the cross section that occurs in the flume could not be represented with any 2D model and this effect could lead some differences in the results obtained with the model and on the experimental flume.

The computational domain is 32 m long and 0.8 m high and the paddle is located in the seaward side of the domain. The computational mesh was divided in three regions of different resolutions, corresponding to the wave generation zone, the breaking zone vicinity and the absorbing zone. The grid was non-uniform in the x-direction, with a minimum cell width, dx , of 1.1 m in the breaking zone and a maximum cell width of 2.9 cm in the generation zone (Figure 8). In the y-direction, the grid was uniform with $dy = 0.55$ cm in the whole domain. The total number of cells was $1903 \times 145 = 27985$. The turbulent model of the COBRAS-UC is based on the $k-\epsilon$ model. Eight numerical gauges were considered in the numerical flume (Figure 8): five located at the same positions as the wave gauges in the physical model, one close to the paddle in order to control the wave generation, four between the paddle and the first experimental gauge position and five more in the positions where ADV measurements were made in the experimental test, to calculate the vertical profile of the horizontal velocity.

Results

Comparison between numerical results and data measured in the physical tests is made for the wave heights and velocities.

First of all, a sensitivity analysis of the initiation parameter of wave breaking was performed. These parameters were varied from 0.45 to 0.7. The calculations were performed for $d = 10\text{cm}$, $T = 1.5\text{sec}$, $H = 8\text{cm}$ on 1/20 back slope.

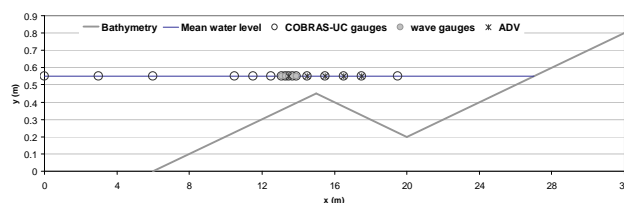


Figure 8. Sketch of wave flume and location of measurement equipment used during the experimental tests and in the numerical simulation.

Figure 9 presents the wave height along the flume computed by the numerical model COULWAVE for each wave breaking parameter tested and the experimental ones.

In general, for wave breaking parameters less than 0.65, the behavior of the wave heights are similar to the experimental ones. However, the maximum experimental value of wave height is not reached by the numerical model. Moreover, after breaking the numerical values are lower than the experimental ones. For wave breakings higher than 0.65, it seems that the wave does not break and the decrease of the wave height is a consequence of the increase of the water depth.

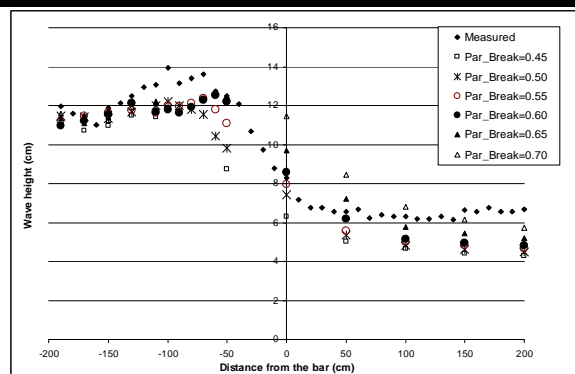


Figure 9. COULWAVE results of wave height. Calculations performed for an incident wave breaking parameter varying between 0.4 to 0.7

From the above and from visual observation, in which was observed that the wave breaks between -100 and -90 cm, the value chosen was 0.55.

Figure 10 displays the comparison of the wave height along the flume between the measurements and the COULWAVE and COBRAS-UC model results.

In general for both models, the wave height behavior along the flume is similar to the one observed in the experimental tests. However, there are some differences between numerical and physical results.

In fact, while the wave heights before the wave breaking agree well for both numerical models with the experimental results, they present smaller values around wave breaking. Moreover, the numerical values become slightly smaller than the experimental ones, especially after 50cm from the bar. Anyway, as expected the RANS model values are closer than the experimental ones.

The disagreement of the numerical and experimental values in the breaking area can be related to the input data on the wave maker. Notice that, in both models, the input conditions on the paddle – significant wave height at COULWAVE model and the

surface elevation and the velocities (vertical and horizontal, which are calculated using Stokes II theory) for COBRAS-UC, are not the same that occur on the experimental flume. In fact, the vertical profile of the input velocities were not measured at the wave maker, so the input velocities could not be compared and that could have influence on the results.

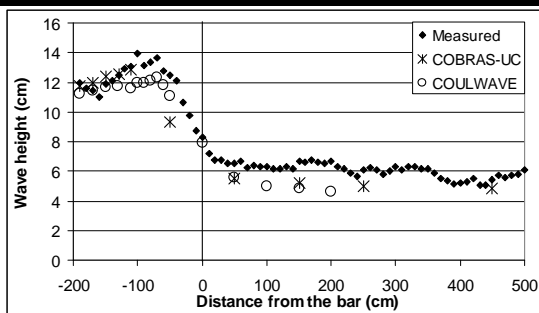


Figure 10. Comparison of wave height between the measured and numerical results (COULWAVE and COBRAS-UC).

Figure 11 displays the comparison of the time series of the horizontal velocity between the measurements and the COBRAS-UC results at $x=-150\text{cm}$, where the wave breaking has not occurred yet. Figure 11(a) shows the record measured at $d=8\text{cm}$. Note that the depth is measured from the still water depth. Due to the free surface at the wave trough and the size of the ADV probe, this is the upper limit in the water column. Figure 11(b) is the record measured at $d=16\text{cm}$, which is very close to the bottom. As shown, the calculation result agrees well for the upper portion of the water column. But in the lower half, the agreement becomes very poor. The reason of disagreement is certainly the same as for the differences in the wave height and it is also due to the improper setting of the bottom boundary conditions. The differences in the initial conditions explain that the result before the wave breaking does not agree very well and also that the horizontal velocity after the wave breaking is not the same. Same as the wave height, the amplitude is smaller than the measured one. The phase information seems to be calculated very well, so the shape of the curve in the record looks similar to the measured one except the amplitude. In the trough region, the disagreement in the lower portion of the water column is not as bad as that in the pre-breaking wave.

SUMMARY

A multi-layered Boussinesq equation model and a RANS model (COBRAS-UC) were tested over simplified bar-trough shaped beaches. The results were compared with the experimental result collected by Okamoto *et al.* (2008). Both models can predict the wave height change very well until the wave breaking initiates. However, it does not agree to the experimental data after the wave breaking initiation. The COBRAS-UC model calculates the horizontal velocity near the free surface very well, but it does not agree to the experimental data in the lower section of the water column.

The main reason for these differences is related to the unknown of the experimental velocity profile at the paddle. Therefore, future work will include the use of a 3D model that can represent the effective flume geometry. This will permit the calculation of a more correct wave heights and velocities (vertical and horizontal) at a chosen point of the flume in the zone when the flume has

constant width. This condition will be the input conditions for COULWAVE and COBRAS-UC models.

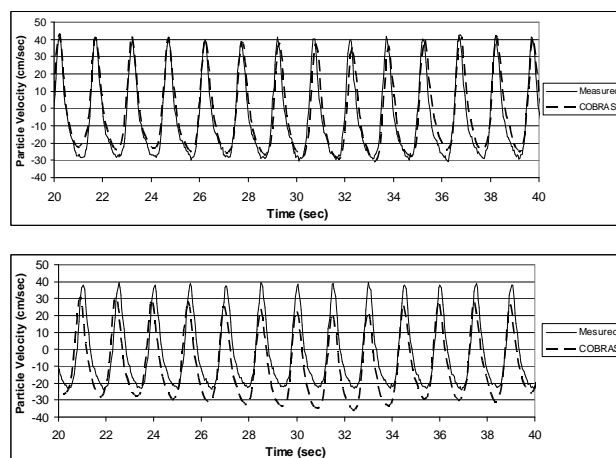


Figure 11. COBRAS-UC and experimental results. Comparison of time series of particle velocity ($x=-150\text{cm}$). (a) $d=8\text{ cm}$ (up); (b) $d=16\text{ cm}$ (down).

ACKNOWLEDGMENTS

This study is funded by the Science and Technology Foundation of the Ministry of Science, Technology and Higher Education, Portugal under the contracts of SFRH/BPD/20508/2004, PTDC/ECM/67411/2006 and PTDC/ECM/73145/2006.

REFERENCES

- DALLY, W.R., R.G., DEAN, and DALRYMPLE, R.A. 1985. Wave height variation across beaches of arbitrary profile, *J. of Geophys. Res.*, Vol. 90, No. C6, Nov. 20, 11, pp. 917-927.
- HSU, T.-J., SAKAKIYAMA, T. and Liu, P.L.-F. 2002. A numerical model for wave motions and turbulence flows in front of a composite breakwater. *Coastal Engineering*, 46, pp. 25-50.
- KENNEDY, A.B., Q. CHEN, J.T. KIRBY, and DALRYMPLE, R.A. 2000. Boussinesq Modeling of Wave Transformation, Breaking and Runup I: 1D. *J. of Waterway, Port, Coastal and Ocean Engineering*, ASCE, Vol. 126, No. 1, January/February, pp. 39-47.
- LARA, J.L., GARCIA, N. and LOSADA, I.J. 2006. RANS modelling applied to random wave interaction with submerged porous structures. *Coastal Engineering*, 53, pp. 395-417
- LIU, P.L.F., LIN, P.Z., CHANG, K.A. and SAKAKIYAMA, T., 1999. Numerical modelling of wave interaction with porous structures. *J. Waterw., Port, Coast., Ocean Eng.*, ASCE 125 (6), pp. 322-330.
- LOSADA, I.J., LARA, J.L., GUANCHE, R. and GONZALEZ-ONDINA, J.M. 2007. Wave overtopping of rubble mound breakwaters. *Coastal Engineering*, submitted.
- LYNETT, P., LIU PL-F. 2004. Modelling wave generation, evolution and interaction with Depth-Integrated, Dispersive Wave equations. COULWAVE Code Manual. Cornell Univ. Long Inter. Wave Modelling Package.
- OKAMOTO, T., FORTES, C.J. and BASCO, D.R. 2008. Wave Breaking Termination on Bar-trough Shaped Beaches. *18th International Offshore and Polar Engineering Conference*, pp. 811-819.